

## Electrochemistry of the Manganese(III)–Manganese(IV) 5,10,15,20-Tetrakis(*p*-trimethylammonio-phenyl)porphyrinate Couple†

Armand Bettelheim,\* Dan Ozer, and Dan Weinraub  
*Nuclear Research Centre-Negev, P.O. Box 9001, Beer Sheva 84190, Israel*

The redox behaviour of the  $[\text{Mn}^{\text{III}}(\text{tmap})] - [\text{Mn}^{\text{IV}}(\text{tmap})]$  couple [tmap = 5,10,15,20-tetrakis-*(p*-trimethylammonio-phenyl)porphyrinate] has been studied in aqueous solutions using cyclic voltammetry, optical transparent electrode thin-layer spectroelectrochemistry, a rotating ring-disc electrode, and differential pulse voltammetry. The couple shows reversible behaviour at  $\text{pH} > 8.5$  with a half-wave potential of +0.04 V at  $\text{pH} 13.4$ . The potential is shifted in a positive direction by 120 mV per decrease of pH unit. The  $[\text{Mn}^{\text{IV}}(\text{tmap})]$  complex is quite stable at high pH values (half-life *ca.* 20 min at  $\text{pH} 13.4$ ) and converts back to the  $\text{Mn}^{\text{III}}$  state with a rate which gradually increases when the solution is acidified. The decomposition of water is described in terms of an electrochemical—chemical catalytic cycle which involves the  $[\text{Mn}^{\text{IV}}(\text{tmap})]$  complex.

It has been determined that manganese is an essential element for the photosynthetic liberation of oxygen from water<sup>1–3</sup> and this is probably linked to the ability of the metal ion to function as a redox catalyst.<sup>4</sup> The oxygen evolving site seems to involve four manganese atoms per photosynthetic unit<sup>5</sup> and the manganese complex is probably *e.s.r.* inactive.<sup>6</sup> Although no conclusive evidence has been obtained regarding the exact nature of such complexes, the donor atoms surrounding the metal will most probably be nitrogen or oxygen (or less likely sulphur) of a prosthetic group or of an apoprotein.<sup>7</sup> Therefore, manganese porphyrins are of potential interest, also because they may possibly play a role in human metabolism.<sup>8</sup> The chemistry of manganese porphyrin and phthalocyanine complexes has been reviewed by Boucher,<sup>9</sup> Smith,<sup>10</sup> Lever,<sup>11</sup> and Harriman.<sup>12</sup>

The solution chemistry of some  $\text{Mn}^{\text{III}} - \text{Mn}^{\text{IV}}$  porphyrin couples has been described by several authors.<sup>13–18</sup> Although the co-ordination chemistry and redox chemistry of  $\text{Mn}^{\text{III}}$  and  $\text{Mn}^{\text{IV}}$  porphyrins have been fairly well characterized, similar studies on  $\text{Mn}^{\text{IV}}$  complexes are scarce.<sup>17–21</sup> The chemical oxidation of manganese(III) hematoporphyrin IX [7,12-bis(1-hydroxyethyl)-3,8,13,17-tetramethylporphyrin-2,18-dipropionic acid] has been achieved using sodium hypochlorite as the oxidizing agent, and the product has been tentatively designated as a  $\text{Mn}^{\text{IV}}$  porphyrin.<sup>20,21</sup> However, the study of the effect of this complex on water oxidation is complicated by a side reaction in which the carboxylic acid side chain of the porphyrin is oxidized to peroxycarboxylic acid or diacetyl peroxide. The electro-oxidation of  $[\text{Mn}^{\text{III}}(\text{tspp})]$  [tspp = 5,10,15,20-tetrakis(*p*-sulphonatophenyl)porphyrinate] and  $[\text{Mn}^{\text{III}}(\text{tmpyp})]$  [tmpyp = 5,10,15,20-tetrakis(1-methyl-4-pyridinio)porphyrinate] has been shown to yield  $\text{Mn}^{\text{IV}}$  complexes for which the stability, the redox potential, and the rate constant for the electrode process depend markedly upon pH.<sup>17</sup> Some  $\text{Mn}^{\text{IV}}$  as well as  $\text{Mn}^{\text{V}}$  porphyrins have also been structurally characterized by *X*-ray crystallography.<sup>22–24</sup>

Electrochemical techniques have been shown to elucidate chemical details of metalloporphyrin systems to which other methods are not sensitive.<sup>25–27</sup> Combined electrochemical, *e.s.r.*, and optical studies have been undertaken to distinguish between metal and ligand oxidation (or reduction) and to

obtain a better correlation between catalytic activities of metalloporphyrins and their redox potentials.<sup>28–30</sup> In a previous publication<sup>15</sup> we reported some electrochemical and spectroscopic properties of the water-soluble porphyrin 5,10,15,20-tetrakis(*p*-trimethylammonio-phenyl)porphyrin ( $\text{H}_2\text{-tmap}$ ) and its  $\text{Mn}^{\text{III}}$  and  $\text{Mn}^{\text{IV}}$  derivatives  $[\text{Mn}^{\text{III}}(\text{tmap})]$  and  $[\text{Mn}^{\text{IV}}(\text{tmap})]$ . In the present study, the electro-oxidation of  $[\text{Mn}^{\text{III}}(\text{tmap})]$  is followed using cyclic voltammetry, differential pulse voltammetry (*d.p.v.*), thin layer coulometry, as well as rotating ring-disc electrode (*r.r.d.e.*) and spectroelectrochemical methods. The catalytic effect on water electro-oxidation is also described.

### Experimental

Solutions were prepared using distilled water. The chloride salt of  $[\text{Mn}^{\text{III}}(\text{tmap})]$ , obtained from Man-Win Chemicals, showed high solubility in aqueous solutions at all pH values. Argon (99.9% pure) was used for deaeration of all solutions.

A glassy carbon–glassy carbon (*g.c.*–*g.c.*) rotating ring-disc electrode (*r.r.d.e.*, Pine Instrument Company) was used. The area of the disc was 0.37  $\text{cm}^2$ . The collection coefficient, determined using the  $[\text{Fe}(\text{CN})_6]^{4-} - [\text{Fe}(\text{CN})_6]^{3-}$  couple was 0.365. The *r.r.d.e.* was pretreated mechanically and electro-chemically. The electrode was polished with alumina powder, washed with a 0.05  $\text{mol dm}^{-3}$   $\text{H}_2\text{SO}_4$  solution and distilled water, and introduced into a 0.1  $\text{mol dm}^{-3}$  KCl argon-saturated solution. The potentials of the disc and ring electrodes were then cycled in the range +0.3 to –0.8 V until a minimum residual current density was obtained (*ca.* 1  $\mu\text{A cm}^{-2}$ ). The same disc electrode was used for the cyclic voltammetry (*c.v.*) experiments.

Spectroelectrochemistry was conducted with the use of an optically transparent thin-layer cell constructed with a gold minigrad working electrode sandwiched between two quartz plates which were separated by Teflon tape spacers along the edges. The pathlength of the thin cell (*ca.* 0.1 mm) was determined by measuring the absorbance of a solution of  $\text{K}_3[\text{Fe}(\text{CN})_6]$  whose concentration had been predetermined in a calibrated 1-cm cell. A Cary 17 spectrophotometer, with a cell compartment modified to permit introduction of electrical leads, was used for the spectropotentiostatic experiments. The optical transparent electrode (*o.t.e.*) thin layer was also used to follow the absorbance in the kinetic experiments.

Cyclic voltammetry and spectroelectrochemistry were performed using a PAR 174A potentiostat coupled with a PAR

† Since the nature of the axial ligands is dependent on the pH, the overall charges of the complexes are omitted throughout.

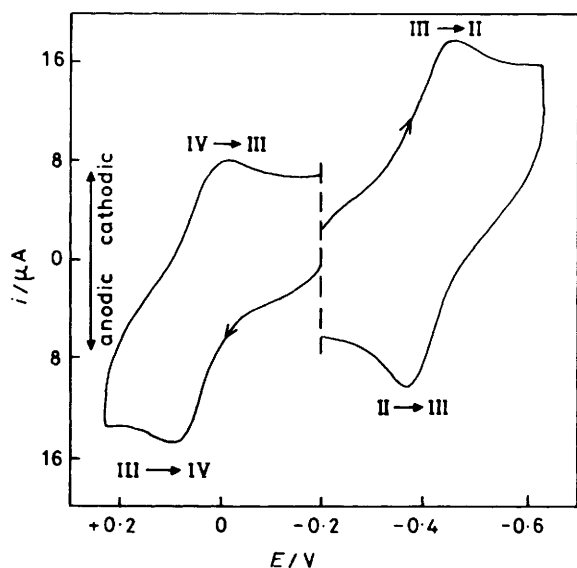


Figure 1. A cyclic voltammogram ( $20 \text{ mV s}^{-1}$ ) for a deaerated  $5 \times 10^{-4} \text{ mol dm}^{-3}$   $[\text{Mn}^{\text{III}}(\text{tmap})]$  solution, also containing  $10^{-2} \text{ mol dm}^{-3}$  phosphate buffer and  $1 \text{ mol dm}^{-3}$  NaCl (pH 13.4)

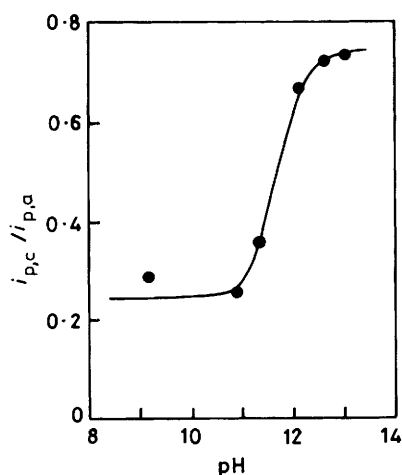


Figure 2. The cathodic-to-anodic peak current ratio as a function of pH (same solution as in Figure 1)

Table. Spectral data of  $\text{Mn}^{\text{II}}$ ,  $\text{Mn}^{\text{III}}$ , and  $\text{Mn}^{\text{IV}}$  (tmap) complexes in solution at pH 13.4

Compound	$\lambda_{\text{max}}/\text{nm}$	$10^{-4}\epsilon/\text{dm}^3 \text{ mol}^{-1} \text{ cm}^{-1}$
$[\text{Mn}^{\text{II}}(\text{tmap})]$	405	5.2
	443	8.2
	572	1.9
	614	1.5
$[\text{Mn}^{\text{III}}(\text{tmap})]$	330–400*	
	461	7
	571	1.9
	606	1.5
$[\text{Mn}^{\text{IV}}(\text{tmap})]$	420	6.7
	555	1.9
	592	1.4

\* Broad absorption band. Two peaks are observed in this region at lower pH (378 and 398 nm at pH 8).

175 sweep generator. The r.r.d.e. experiments were performed using a double potentiostat (Pine Instrument Company) and differential pulse voltammetry (d.p.v.) using a PAR 173 polarograph.

All reported potentials are with respect to a saturated calomel electrode (s.c.e.). Experiments were conducted at room temperature ( $20 \pm 1^\circ \text{C}$ ).

## Results and Discussion

Figure 1 shows a c.v. curve obtained for a polished g.c. electrode placed in a deaerated solution containing  $5 \times 10^{-4} \text{ mol dm}^{-3}$   $[\text{Mn}^{\text{III}}(\text{tmap})]$  and adjusted to pH 13.4. When the potential is scanned in the negative direction, a couple appears at ca.  $-0.4 \text{ V}$ . The reduction of  $[\text{Mn}^{\text{III}}(\text{tmap})]$  to  $[\text{Mn}^{\text{II}}(\text{tmap})]$  at this potential has been described in a previous publication.<sup>15</sup> However, as can be seen from Figure 1, c.v. in the positive potential direction ( $-0.2$  to  $+0.3 \text{ V}$ ) reveals another electrode reaction. The waves are well defined, and at a scan rate of  $5\text{--}50 \text{ mV s}^{-1}$ , the peak separation between the anodic and cathodic potentials ( $E_{p,a}$  and  $E_{p,c}$  respectively) is  $60 \pm 2 \text{ mV}$  and it increases to  $75 \text{ mV}$  at a scan rate of  $200 \text{ mV s}^{-1}$ . These  $\Delta E_p$  values are close to that expected for a reversible one-electron oxidation of  $[\text{Mn}^{\text{III}}(\text{tmap})]$ . Assuming conversion to the  $\text{Mn}^{\text{IV}}$  state under these conditions, as already suggested for another porphyrin,<sup>20,21</sup> the anodic process is assigned to a  $[\text{Mn}^{\text{III}}(\text{tmap})] \rightarrow [\text{Mn}^{\text{IV}}(\text{tmap})]$  transition with  $E_{\frac{1}{2}} [= (E_{p,a} - E_{p,c})/2]$  of  $+0.04 \text{ V}$  at pH 13.4. The peak current, for  $[\text{Mn}^{\text{III}}(\text{tmap})]$  oxidation at a constant scan rate, is linearly proportional to the complex concentration and it is proportional to the square root of the scan rate,  $v^{\frac{1}{2}}$ , when the complex concentration is held constant. These results are in agreement with the Randles-Sevcik equation for a diffusion-controlled process.<sup>31</sup> The diffusion coefficient was estimated using this equation to be  $(1.0 \pm 0.1) \times 10^{-6} \text{ cm}^2 \text{ s}^{-1}$ , similar to that cited in the literature for a similar porphyrin.<sup>32</sup>

Decreasing the pH from 13 to 8.5 causes the following changes: (a)  $E_{\frac{1}{2}}$  shifts to more positive values at an approximate rate of  $120 \text{ mV}$  per decrease of pH unit, indicating an oxidation which involves two protons per electron; (b) the cathodic to anodic peak current ratio ( $i_{p,c}/i_{p,a}$ ) gradually decreases, indicating that the oxidation product of  $[\text{Mn}^{\text{III}}(\text{tmap})]$  is stable only at high pH (Figure 2).

Cyclic voltammetry at pH  $< 8.5$  yielded unsatisfactory results due to the low stability of the oxidation product causing very large potential peak separations and gradual disappearance of the cathodic peaks.

Further characterization of the anodic product has been studied by thin-layer spectroelectrochemistry using a gold minigrad electrode. Coulometric experiments, conducted  $200 \text{ mV}$  more positive or negative than the  $E_{\frac{1}{2}}$  value at pH 13.4, confirm one-electron oxidation/reduction of the manganese(III) ion. During incremental oxidation of  $[\text{Mn}^{\text{III}}(\text{tmap})]$ , the  $461 \text{ nm}$  peak of  $\text{Mn}^{\text{III}}$  diminishes and a peak at  $420 \text{ nm}$  appears. The main absorption maxima and absorption coefficients of the various oxidation states of the manganese porphyrin are listed in the Table. The electronic spectrum of  $[\text{Mn}^{\text{IV}}(\text{tmap})]$  is similar to that of manganese(IV) hematoporphyrin IX, for which the absorptions have been assigned to  $\pi\text{--}\pi$  and ligand-to-metal charge-transfer transitions for the high and low energy bands, respectively.<sup>9</sup>

The absorbance at  $461 \text{ nm}$  has been followed while the potential has been stepped from a value cathodic enough to produce  $[\text{Mn}^{\text{II}}(\text{tmap})]$  ( $-0.6 \text{ V}$ ), to a potential which produces  $[\text{Mn}^{\text{IV}}(\text{tmap})]$  ( $+0.3 \text{ V}$ ). The behaviour of the absorbance which characterizes the  $\text{Mn}^{\text{III}}$  complex (Figure 3) indicates that no direct two-electron oxidation or reduction  $\text{Mn}^{\text{II}} \rightleftharpoons \text{Mn}^{\text{IV}}$  can be achieved. In the two cases  $\text{Mn}^{\text{III}}$  is formed as an

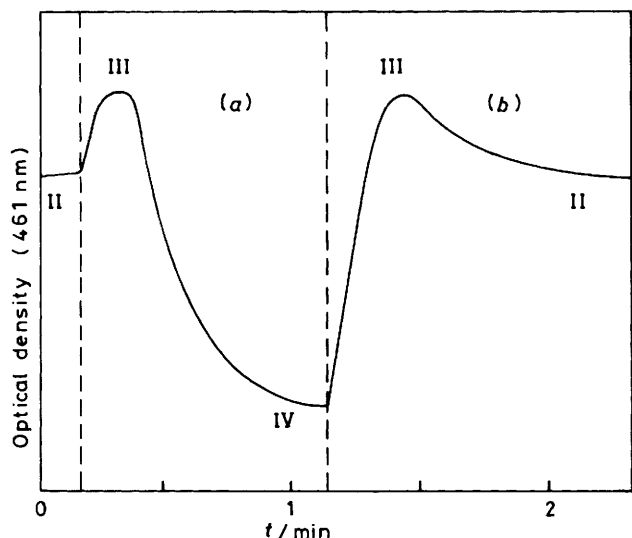


Figure 3. The absorbance at 461 nm as a function of time when the potential is stepped (a) from  $-0.6$  to  $+0.3$  V and (b) from  $+0.3$  to  $-0.6$  V (same solution as in Figure 1)

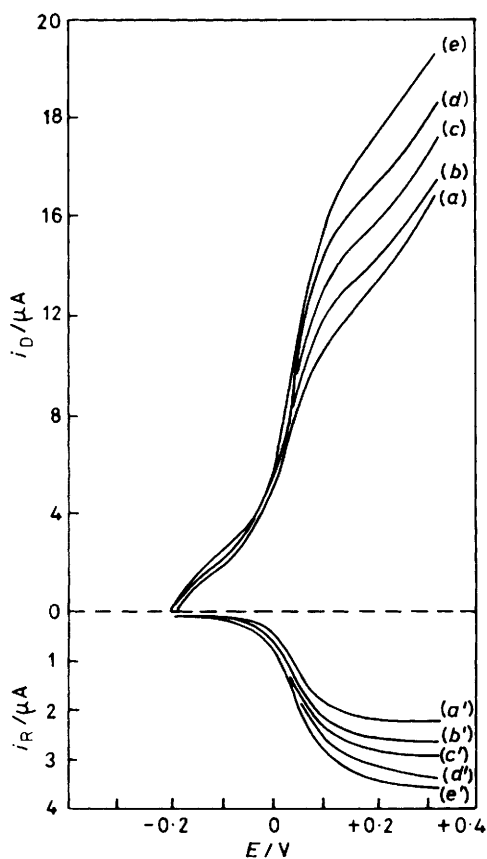


Figure 4. R.r.d.e. voltammograms (ring potential = 0 V, scan rate of the disc potential =  $2 \text{ V min}^{-1}$ ) for the same solution as in Figure 1. Rotation speeds are 200, 400, 600, 800, and 1000 r.p.m. for curves (a)–(e) respectively

intermediate. The results suggest a favourable reaction between  $[\text{Mn}^{\text{IV}}(\text{tmap})]$  and  $[\text{Mn}^{\text{II}}(\text{tmap})]$  to yield  $[\text{Mn}^{\text{III}}(\text{tmap})]$ .

When the applied potential to form  $[\text{Mn}^{\text{IV}}(\text{tmap})]$  is interrupted, a gradual optical density (o.d.) decrease of the band at 420 nm and an increase of the peak at 461 nm are indicative of a conversion of  $[\text{Mn}^{\text{IV}}(\text{tmap})]$  back to  $[\text{Mn}^{\text{III}}(\text{tmap})]$ .

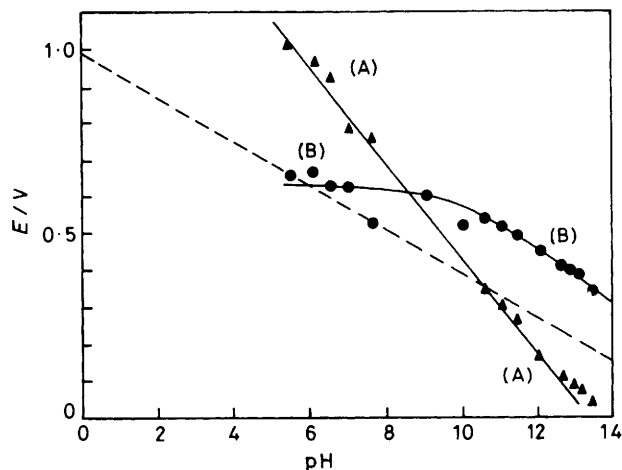


Figure 5. Potentials of peaks (A) and (B) as obtained from d.p.v. as a function of pH. The dashed curve represents the theoretical oxidation potential of water as a function of pH

Moreover, the conversion rate can be determined following these o.d. changes. Plots of  $\log \Delta \text{o.d.}$  vs. time are linear, indicating that the reaction is first order with respect to  $[\text{Mn}^{\text{IV}}(\text{tmap})]$ . The slopes for the concentration decrease of  $\text{Mn}^{\text{IV}}$  and increase of  $\text{Mn}^{\text{III}}$  are identical. The rate constant is  $(6 \pm 0.8) \times 10^{-4} \text{ s}^{-1}$  at pH 13.4. No significant change ( $\pm 20\%$ ) is observed at pH 12, while a five-fold increase is found at pH 10.3  $[(3.2 \pm 0.5) \times 10^{-3} \text{ s}^{-1}]$ . The rate constants at lower pH values have not been evaluated due to irreversible absorbance changes.

The oxidation of  $[\text{Mn}^{\text{III}}(\text{tmap})]$  has also been studied using a g.c.-g.c. rotating ring-disc electrode (r.r.d.e.). Typical r.r.d.e. voltammograms are shown in Figure 4. Curves (a)–(e) represent the disc currents ( $i_{\text{D}}$ ) obtained at different rotation speeds when the potential is scanned in the positive direction. The half-wave potential of  $[\text{Mn}^{\text{III}}(\text{tmap})]$  oxidation at pH 13.4,  $E_{\frac{1}{2}} + 0.04$  V, correlates well with that found in the c.v. experiments. However, the limiting currents are not proportional to the square root of the rotation rate. The deviation from linearity may reflect the intervention of a potential-independent chemical step as the current-limiting factor [reaction (3), see later].

The ring potential is set at 0 V to monitor the  $\text{Mn}^{\text{IV}}$  complex formed at the disc. Curves (a')–(e') in Figure 4 represent the ring currents ( $i_{\text{R}}$ ) as a function of the disc potential. The ratio  $i_{\text{R}}/i_{\text{D}}$  is 0.28 and is independent of rotation speed. Since the collection coefficient of the r.r.d.e. has been determined (using the  $[\text{Fe}(\text{CN})_6]^{4-}-[\text{Fe}(\text{CN})_6]^{3-}$  couple) to be ca. 0.4, this corresponds to a  $[\text{Mn}^{\text{III}}(\text{tmap})]$  oxidation yield of ca. 70% at pH 13.4. The same yield is obtained at pH 12, in good agreement with the invariance of the c.v. cathodic-to-anodic peak current ratio in this pH range (Figure 2). The r.r.d.e. technique does not supply additional information at lower pH due to the non-well defined shape of the disc voltammograms and to the very low ring currents. These results are in agreement with the conclusions of the c.v. and spectroelectrochemical measurements:  $[\text{Mn}^{\text{IV}}(\text{tmap})]$  is quite stable only at pH  $> 12$ .

Two oxidation peaks with  $E_{\text{p}} + 0.035$  (A) and  $+0.335$  V (B) are observed using the d.p.v. method for a g.c. electrode in a  $[\text{Mn}^{\text{III}}(\text{tmap})]$  solution at pH 13.4. The first corresponds to that found by the other electrochemical techniques. The second is revealed only by d.p.v., probably due to the close vicinity to the foot of the wave corresponding to water oxidation. From Figure 5, it can be seen that while the potential of the first peak (A) increases 120 mV per decrease of pH unit, the slope of the

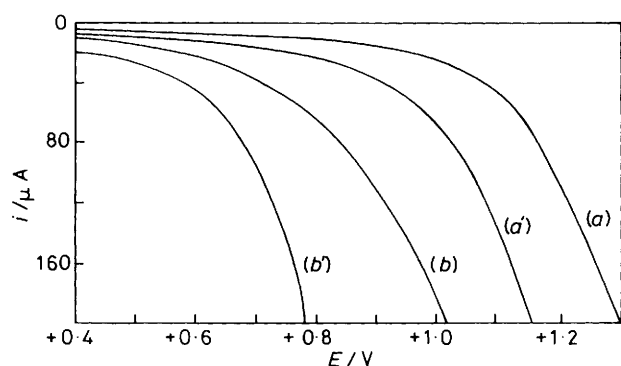
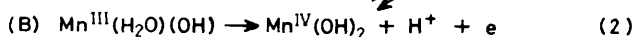
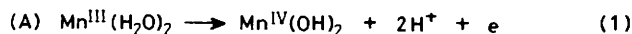


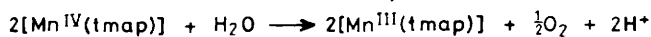
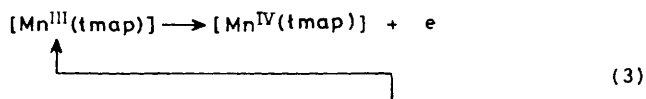
**Figure 6.** Polarization curves for electro-oxidation of water in a solution containing  $10^{-2}$  mol  $\text{dm}^{-3}$  phosphate buffer and 1 mol  $\text{dm}^{-3}$  NaCl at pH 5 (a) and 13 (b). Curves (a') and (b') are obtained at pH 5 and 13 respectively, in the presence of  $5 \times 10^{-4}$  mol  $\text{dm}^{-3}$   $[\text{Mn}^{\text{III}}(\text{tmap})]$

second (B) is *ca.* 60 mV per decrease of pH unit. This corresponds to two electrodic reactions involving two and one proton per electron, respectively [equations (1) and (2)].



The  $\text{p}K_a$  of the aqueous hydrolysis of  $[\text{Mn}^{\text{III}}(\text{tmap})]$  has been previously estimated from spectrophotometric titrations to be  $11.4 \pm 0.3$ .<sup>15</sup> The  $\text{p}K_a$  of the acid-base equilibrium of  $[\text{Mn}^{\text{IV}}(\text{tmap})]$  has not been determined. However, it has been suggested for a similar porphyrin that the great acidity ( $\text{p}K_a < 10$ ) of the co-ordinated water protons results from the high positive charge of the  $\text{Mn}^{\text{IV}}$  species.<sup>9</sup> The  $[\text{Mn}^{\text{IV}}(\text{tmap})]$  complex, which has been spectroelectrochemically characterized and which is relatively stable at high pH values, is probably the complex which is co-ordinated with two hydroxide ions.

Polarization curves obtained at a g.c. electrode in the positive potential range are shown in Figure 6. When the potentials of water oxidation in phosphate buffer at low and high pH [curves (a) and (b)] are compared to those obtained for the same solutions in the presence of  $[\text{Mn}^{\text{III}}(\text{tmap})]$  [curves (a') and (b')], it can be concluded that the water oxidation overpotential is decreased by *ca.* 200 mV. This is in agreement with the results described in Figure 5: the potentials of the two  $\text{Mn}^{\text{III}}$  species are more positive than the theoretical potential of water oxidation. Moreover, water decomposition at high and low pH occurs at potentials close to those of peaks (A) and (B) [see equilibria (1) and (2)], respectively. As already suggested for the  $[\text{Cu}^{\text{III}}(\text{tmap})]$ – $[\text{Cu}^{\text{II}}(\text{tmap})]$  couple,<sup>32</sup> the results seem to indicate that water decomposition is essentially determined by an electrochemical–



chemical (e.c.) catalytic mechanism [reaction (3)], where  $[\text{Mn}^{\text{III}}(\text{tmap})]$  is oxidized at the electrode to  $[\text{Mn}^{\text{IV}}(\text{tmap})]$  which is unstable, particularly at low pH, and reacts with water

\* The redox potential of  $\text{H}_2\text{O}$ – $\text{O}_2$  at pH 13 ( $E = +0.21$  V) is more positive than that of  $[\text{Mn}^{\text{III}}(\text{tmap})]$ – $[\text{Mn}^{\text{IV}}(\text{tmap})]$ , therefore it is more likely that  $\text{H}_2\text{O}$ – $\text{H}_2\text{O}_2$  is involved in reaction (3), with  $\text{H}_2\text{O}_2$  being catalytically dismutated to water and oxygen.

to regenerate the  $[\text{Mn}^{\text{III}}(\text{tmap})]$  complex.\* Not only oxygen but also other gases (such as  $\text{Cl}_2$ ) may be evolved and further study is required to determine the products under various experimental conditions.

## Conclusions

The electrochemical results are considered to demonstrate that the water soluble complex  $[\text{Mn}^{\text{III}}(\text{tmap})]$  undergoes a one-electron oxidation of the manganese ion. In addition to metal oxidation, it is possible to oxidize the porphyrin ligand, *i.e.* remove an electron from a  $\pi$  orbital, and form a porphyrin radical. This has been shown for a number of metalloporphyrins in aprotic solvents.<sup>28</sup> E.s.r. measurements have not yet been performed; however, it is unlikely that such radicals are stable in aqueous solutions on the time-scale of the electrochemical experiments. The relatively high stability of the oxidized  $[\text{Mn}^{\text{IV}}(\text{tmap})]$  complex, particularly at high pH (half-life of *ca.* 20 min at pH 13.4), suggests a metal ion oxidation.

Cyclic voltammetry shows reversible behaviour for the  $[\text{Mn}^{\text{III}}(\text{tmap})]$ – $[\text{Mn}^{\text{IV}}(\text{tmap})]$  couple at pH 8.5–13.4. The half-wave potential of this couple at pH 13.4, as found using cyclic voltammetry as well as the r.r.d.e. technique, is +0.04 V and increases by 120 mV per decrease of pH unit. Differential pulse voltammetry reveals another oxidation reaction at a potential of +0.335 V and with a slope of 60 mV per pH unit. The two anodic reactions are suggested to involve two  $[\text{Mn}^{\text{III}}(\text{tmap})]$  species, present in an acid–base equilibrium.

The importance of manganese in sustaining the capacity of biological material to carry out photosynthesis has been described in the literature<sup>33,34</sup> as being a consequence of its role as a manganese porphyrin protein complex whose +4 oxidation state can oxidize oxide ions in water to molecular oxygen. Even though the products of the oxidizing effect of the  $[\text{Mn}^{\text{IV}}(\text{tmap})]$  complex on water have not been identified, the spectroelectrochemical results indicate that  $[\text{Mn}^{\text{IV}}(\text{tmap})]$  is unstable in solution and reverts to the  $\text{Mn}^{\text{III}}$  derivative. The first-order rate constant for spontaneous reduction at pH 13.4 is increased by a factor of five when the pH is decreased to 10.3. The electrocatalytic electro-oxidation of water is proposed to occur through an e.c. mechanism, similar to that suggested for the effect of  $[\text{Cu}^{\text{III}}(\text{tmap})]$ .<sup>32</sup>

## References

- 1 E. Kessler, W. Arthur, and J. E. Bruger, *Arch. Biochem. Biophys.*, 1957, **71**, 326.
- 2 G. Englesma, A. Yamamoto, E. Markham, and M. Calvin, *J. Phys. Chem.*, 1962, **66**, 2517.
- 3 R. B. Park and J. Biggins, *Science*, 1964, **144**, 1009.
- 4 M. Calvin, *Rev. Pure Appl. Chem.*, 1965, **15**, 1.
- 5 G. M. Cheniae and I. F. Martin, *Biochim. Biophys. Acta*, 1970, **197**, 219.
- 6 R. E. Blankenship and K. Sauer, *Biochim. Biophys. Acta*, 1974, **357**, 252.
- 7 G. M. Cheniae and I. F. Martin, *Biochim. Biophys. Acta*, 1968, **153**, 819.
- 8 D. C. Borg and G. C. Catzias, *Nature (London)*, 1958, **182**, 1677.
- 9 L. J. Boucher, *Coord. Chem. Rev.*, 1972, **7**, 289.
- 10 K. M. Smith, 'Porphyrins and Metalloporphyrins,' Elsevier, New York, 1975.
- 11 A. B. P. Lever, *Adv. Inorg. Chem. Radiochem.*, 1965, **27**.
- 12 A. Harriman, *Coord. Chem. Rev.*, 1979, **28**, 147.
- 13 L. J. Boucher and H. K. Garber, *Inorg. Chem.*, 1970, **9**, 2644.
- 14 D. J. Davis and J. G. Montalvo, *Anal. Chem.*, 1969, **41**, 1195.
- 15 A. Bettelheim, D. Ozer, and R. Parash, *J. Chem. Soc., Faraday Trans. 1*, 1983, 1555.
- 16 P. Hambright and R. F. X. Williams, 'Porphyrin Chemistry Advances,' ed. F. R. Longo, Ann Arbor Science, Michigan, 1979, p. 284.

- 17 A. Harriman, *J. Chem. Soc., Dalton Trans.*, 1984, 141.  
18 K. Kalyanasundaram and M. Neumann-Spallart, *J. Phys. Chem.*, 1982, **86**, 5163.  
19 N. Carnieri, A. Harriman, and G. Porter, *J. Chem. Soc., Dalton Trans.*, 1982, 1231.  
20 P. A. Loach and M. Calvin, *Biochemistry*, 1963, **2**, 361.  
21 P. A. Loach and M. Calvin, *Biochim. Biophys. Acta*, 1964, **79**, 379.  
22 B. C. Schradt, F. J. Hollander, and C. L. Hill, *J. Chem. Soc., Chem. Commun.*, 1981, 765.  
23 B. C. Schradt, F. J. Hollander, and C. L. Hill, *J. Am. Chem. Soc.*, 1982, **104**, 3964.  
24 C. L. Hill and F. J. Hollander, *J. Am. Chem. Soc.*, 1982, **104**, 7318.  
25 D. G. Davis and D. J. Orgeron, *Anal. Chem.*, 1966, **38**, 179.  
26 D. G. Davis and R. F. Martin, *J. Am. Chem. Soc.*, 1966, **88**, 1365.  
27 T. M. Bednarski and J. Jordan, *J. Am. Chem. Soc.*, 1967, **89**, 1552.  
28 A. Wolberg and J. Manassen, *J. Am. Chem. Soc.*, 1970, **92**, 2982.  
29 J. Manassen and A. Bar-Ilan, *J. Catal.*, 1970, **17**, 86.  
30 J. Manassen, *Catal. Rev. (Science and Engineering)*, 1974, 223.  
31 J. E. Randles, *Trans. Faraday Soc.*, 1948, **44**, 327; A. Sevcik, *Collect. Czech. Chem. Commun.*, 1948, **13**, 349.  
32 A. Bettelheim, D. Ozer, and R. Harth, *J. Chem. Soc., Faraday Trans. 1*, 1985, 1577.  
33 J. H. Wang, *Acc. Chem. Res.*, 1970, **3**, 90.  
34 J. M. Olson, *Science*, 1970, **168**, 438.

Received 3rd June 1985; Paper 5/940